Heat-Driven Release of a Drug Molecule from Carbon Nanotubes: A Molecular Dynamics Study

Vitaly V. Chaban,[†] Timur I. Savchenko,[‡] Sergiy M. Kovalenko,[‡] and Oleg V. Prezhdo*[,†]

Department of Chemistry, University of Rochester, Rochester, New York 14627, and National University of Pharmacy, Kharkiv, Ukraine

Received: May 18, 2010; Revised Manuscript Received: August 1, 2010

Hydrophobicity and the ability to absorb light that penetrates through living tissues make carbon nanotubes (CNTs) promising intracellular drug delivery agents. Following insertion of a drug molecule into a CNT, the latter is delivered into a tissue, is heated by near-infrared radiation, and releases the drug. To assess the feasibility of this scheme, we investigate the rates of energy transfer between CNT, water, and the drug molecule and study the temperature and concentration dependence of the diffusion coefficient of the drug molecule inside CNTs. We use ciprofloxacin (CIP) as a sample drug: direct penetration of CIP through cell membranes is problematic due to its high polarity. The simulations show that a heated CNT rapidly deposits its energy to CIP and water. All estimated time scales for the vibrational energy exchange between CNT, CIP, and water are less than 10 ps at 298 K. As the system temperature grows from 278 to 363 K, the diffusion coefficient of the confined CIP increases 5−7 times, depending on CIP concentration. The diffusion coefficient slightly drops with increasing CIP concentration. This effect is more pronounced at higher temperatures. The simulations support the idea that optical heating of CNTs can assist in releasing encapsulated drugs.

Introduction

Delivery of synthetic drugs to a given target area in a living organism constitutes a crucial medical problem. Penetration through the cell membrane often presents serious difficulties; in particular, polar drug molecules prefer to remain hydrated and avoid the hydrophobic environment of lipid bilayers. In this context, transport systems providing specific drug delivery mechanisms are of great practical interest, since they can substantially increase the effectiveness of medical treatments. Recently, it was shown that carbon nanotubes (CNTs) readily penetrate into biological cells[1] and that their functionalization, either covalent or noncovalent, ensures simultaneously high biological accessibility[2−5] and low toxicity.[1,6] In combination with the unique CNT chemical structure, these properties favor development of new transport systems based on CNTs. It was recently shown successfully[7] that both inner and outer surfaces of nanotubes could be used for drug delivery. In the experiments, drug molecules were attached to CNTs covalently with biologically degradable bonds[8] and noncovalently via surfactants adsorbed on CNTs[9] and by direct adsorption onto the CNT surface.[10] Gradual release of the drug cargo could be achieved by destruction of the labile chemical bond with intracellular enzymes. Enzymes can be used to destroy biodegradable CNT capping agents.[11] The drug could be kept in the inner cavity of the nanotube for a long time and slowly be emitted by self-diffusion.[12,13]

In vitro and in vivo experiments have demonstrated that CNT transport systems could be used for delivering a variety of compounds, including nucleic acids;[14−16] proteins;[8,10,16,17] the anticancer agents cisplatin,[8,9] doxorubicin,[18] and paclitaxel;[19] the antibacterial agent amphotericin B;[20] the anti-inflammatory steroid dexamethasone;[21] etc. To increase the interaction selectivity, ligands to the membrane receptors of the target cells were widely utilized.

Given the choice between drug storage inside and outside CNTs, both of which have been demonstrated experimentally, the CNT inner cavity appears more preferable. Such a scheme avoids multistage syntheses, reliably defends drugs from the destructive chemical action of cell enzymes, and leads to universal delivery systems that can be used with essentially any drug molecule, independent of its particular chemical structure. At this point, development of a well-performing mechanism for drug release from inside CNTs becomes a major challenge. The proposed nanosyringe[7,22] must contain a piston inside the tube. Ferromagnets[23] and CNTs with smaller diameters[24] were suggested for this purpose. Generally, such devices are quite complex and have not yet been created in practice.

An additional property of CNTs that carries great value and can be utilized for drug delivery is their ability to absorb near-infrared (NIR) radiation, covering the spectral window of 800−1100 nm.[25] The biological value of this particular CNT property arises due to the fact that most living organisms are transparent to NIR radiation.[26] Recently, it was successfully shown that a NIR laser could be used to heat and destroy cancer cells that had been previously equipped with CNTs.[27] Using a milder light intensity, NIR radiation allowed the scientists to release DNA molecules from DNA-functionalized CNTs without causing cell death.[27]

Several simulations of CNT-based drug delivery and release systems were recently performed by classical molecular dynamics.[7,24] For instance, ref 24 showed that a peptide encapsulated inside a CNT or attached to the outer surface of the CNT can be released by another nanotube through a competitive replacement process. The release is driven by van der Walls interactions. A review of the computer simulations of the CNT drug delivery systems is provided by ref 7.

* Corresponding author. E-mail: prezhdo@chem.rochester.edu.
[†] University of Rochester.
[‡] National University of Pharmacy, Kharkiv.

10.1021/jp104507g
Published on Web 09/10/2010

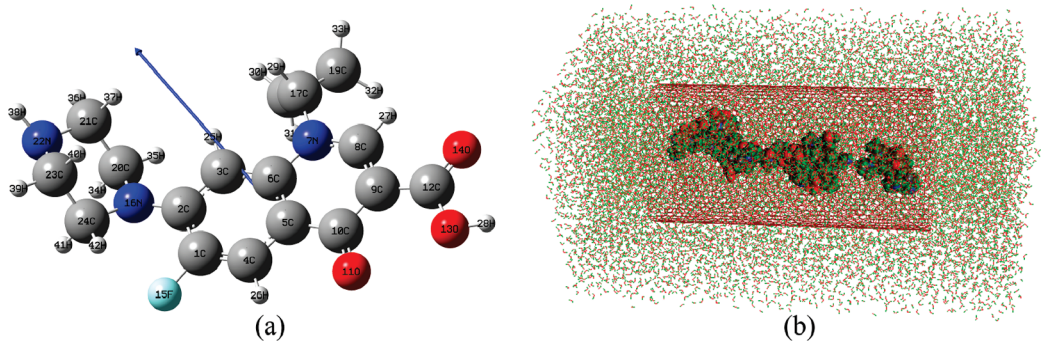

Figure 1. (a) Optimized geometry of the ciprofloxacin molecule. The atom numbers correspond to those in Table 2. The blue arrow shows the direction of the dipole moment, whose magnitude is 13.9 D. (b) System II after the equilibration stage. See Table 1 for the system definition. CIP molecules are shown as "spheres" whereas all other particles are shown as "sticks".

TABLE 1: Simulated Systems Consisting of a Carbon Nanotube (CNT), N_{water} Water Molecules, and N_{CIP} CIP Molecules[a]

N	CNT	N_{water}	N_{CIP}	Density, kg/m^3
I	(14, 14)	2 290	1	1164 ± 1
II	(30, 30)	16 071	10	1117 ± 2
III			15	1121 ± 2
IV			20	1122 ± 2
V			30	1130 ± 2

[a] The system densities are given for 298 K.

TABLE 2: Coulomb Charges of the Ciprofloxacin Molecule Calculated Ab Initio and Used in the Molecular Dynamics Simulation[a]

site	charge, e	site	charge, e	site	charge, e
1C	+0.221 961	15F	−0.243 679	29H	+0.039 190
2C	+0.055 382	16N	−0.111 246	30H, 31H	+0.067 605 5
3C	−0.089 181	17C	+0.306 136	32H, 33H	+0.252 607 5
4C	−0.194 750	18C	+0.043 211	34H	+0.065 977
5C	−0.041 791	19C	−0.718 730	35H	+0.013 564
6C	−0.130 399	20C	+0.055 448	36H, 37H	+0.055 451 5
7N	0.063 498	21C	+0.145 614	38H	+0.394 600
8C	−0.117 160	22N	−0.832 260	39H	+0.059 893
9C	−0.177 274	23C	+0.169 804	40H	+0.036 976
10C	0.545 958	24C	−0.169 448	41H	+0.109 269
11O	−0.663 625	25H	+0.034 855	42H	+0.130 633
12C	+0.656 204	26H	+0.182 392		
13O	−0.574 855	27H	+0.180 033		
14O	−0.631 961	28H	+0.434 432		

[a] See Figure 1a for site designations.

The present work investigates the effect of CNT heating by NIR-radiation on a drug molecule encapsulated inside the tube. The excess energy delivered to the CNT by a NIR light can be used to accelerate the diffusion of the molecule inside the tube and its release from the tube. It can also be used to weaken and break the CNT−molecule interaction. By adjusting the NIR radiation intensity, one can control the local temperature around the nanotubes and avoid destruction of the target biological cell.

The reported study is performed using a series of molecular dynamics (MD) simulations with ciprofloxacin (CIP) as a drug. The structure of the CIP molecule, Figure 1a, is common to all fluoroquinolone antibiotics. Nowadays, medicines of this class are widely used in clinical practice for healing infections of different degrees of localization.[28] The simulations allow us to obtain the rates of energy transfer between the CNT, CIP, and water and to evaluate the diffusion coefficient for CIP inside CNTs over a range of temperatures and CIP concentrations. The simulations support the idea that optical heating of CNTs can be used for release of encapsulated drugs and provide valuable details of this process.

Computational Method.

Force Fields. The GROMACS[29] program was used to perform MD simulations on several systems containing CNT, CIP, and water. The exact composition of all systems is presented in Table 1. Figure 1b shows an example of the simulation cell. The all-atom GROMOS96 force field[30] was selected to represent all bonded and nonbonded interactions. This force field is among the most successful ones so far. It was developed primarily for the simulation of the large organic molecules and has been thoroughly tested. Broadly speaking, CNTs can be regarded as large organic molecules, as well. The cross-term Lennard-Jones (12, 6) parameters were obtained using the Lorenz-Berthelot combination rules.[33]

The partial charge distribution on the water molecule corresponded to the SPCE model,[31] whereas the flexible carbon nanotubes were held electrostatically neutral. The charges on the CIP molecule are listed in Table 2. They were determined by the electrostatic potential fit using the CHELPG scheme.[32] The scheme was applied to the results of the density functional theory (B3LYP/aug-cc-pVDZ) ab initio electronic structure calculation for CIP in water. Water was represented implicitly with a polarizable continuum model. The charges on equivalent hydrogens were averaged. The dipole moment of CIP obtained by the ab initio calculation is 13.9 D.

It was found for the CIP−water and CIP−CIP interactions that the Lennard-Jones contribution to the interaction energy, defined in the GROMOS96 force field, was small compared with the Coulomb contribution. Thus, the details of the GROMOS96 force field were important only for the CNT−water and CNT−CIP interactions. The CIP−water and CIP−CIP interactions, dominated by the Coulomb charges, were described by the ab initio model.

Simulation Details. The simulated systems consisted of a CNT located in the center of the MD simulation cell surrounded by 3−4 layers of bulk water to properly represent the Coulomb part of the interaction energy between the confined solution and its bulk phase. Initially, the CIP molecules were located inside the CNTs, representing the situation in which the tube had already been delivered to the target cell, but had not been unloaded yet. Both single and multiple CIP molecules were considered inside the tubes. The number of molecules was varied to represent different CIP concentrations. During the initialization process, multiple CIP molecules were placed uniformly inside the CNTs to minimize the total energy of the confined solution. During the 2 ns equilibration stage, all degrees of freedom of the CIP molecules were kept frozen while SPCE water and flexible mobile CNTs were relaxed. This protocol

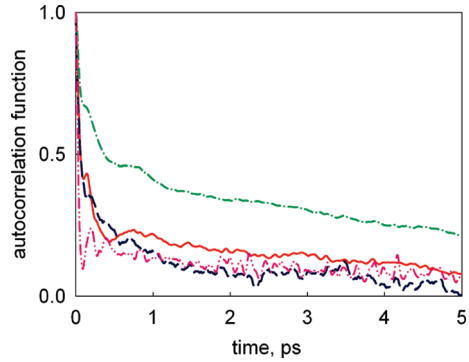

Figure 2. Normalized autocorrelation functions of the energies of interaction between the following components of system I (see Table 1): CNT−-CIP (solid red line), CNT−water (dashed−dotted green line), CIP−water, Coulomb interaction (dashed blue line), and CIP−water, Lennard-Jones interaction (dashed−dotted−dotted pink line).

was adopted to maintain the initial CIP concentration inside the CNTs. After the first 2 ns equilibration stage, the CIP molecules were released, and an additional 200 ps equilibration was performed. The properties of interest were calculated during a 1 ns production run, following the equilibration stage. A 1 fs MD time step was employed. The nonbonded forces were represented with a shifted force correction applied between 0.9 and 1.0 nm, and the Coulomb interactions were computed using the reaction-field-zero method.[34] Constant temperature and pressure were maintained using the velocity rescaling thermostat[34] and a Parrinello−Rahman barostat[35] with the 1 ps characteristic time for each of them. The pressure was equal to 1 bar in all simulations. Six temperatures were used: 278, 298, 310, 348, and 363 K (see Table 1). Periodic boundary conditions consistent with the simulation cells were employed.

System Details. Two (14, 14) and (30, 30) armchair CNTs with small and intermediate diameters were considered. Namely, their diameters were ∼2 and 4 nm, respectively. The lengths of both CNTs were chosen to be 8 nm. The (14, 14) CNT was used to simulate the drug delivery system containing a single confined drug molecule, whereas the (30, 30) CNT was chosen to allow confinement of a considerable number of CIPs, up to 30 molecules. Four different drug loading levels were considered, ranging from 10 to 30 molecules per CNT (see Table 1). Overall, 30 separate MD simulations were performed, including five systems at six temperatures each.

Data Analysis. The MD trajectories were used to calculate the CIP self-diffusion coefficients and the autocorrelation functions (ACFs) for the pairwise interactions among CNT, CIP, and water. The ACFs were computed to evaluate the time scales of energy exchange between these three subsystems.

The ACFs of the pairwise interaction energies between CNT, CIP, and water were computed according to the following equation,

$$C_{EE}(t) = \langle E(0)\, E(t)\rangle \tag{1}$$

in which the angular brackets represent canonical averaging. Since the CNTs were electrostatically neutral, their interaction with water and CIP molecules included only the Lennard-Jones (12, 6) term. On the contrary, water and CIP interacted via both Coulomb and Lennard-Jones parts, which were studied separately for comparison.

The calculated ACFs could be well approximated by the biexponential function (Figure 2),

$$C_{EE}(t) = A\cdot\exp(-t/\tau_{fast}) + (1 - A)\cdot\exp(-t/\tau_{slow}) \tag{2}$$

Here, the first and second terms describe the fast and slow time scales of the energy exchange, and A gives the amplitude of the fast component. Correspondingly, $(1 - A)$ is the amplitude of the slow energy exchange component.

The mobility of the drug molecules were estimated at different temperatures and concentrations by computing the diffusion coefficients. They were calculated using the Green−Kubo[32] relationship involving the ACFs of the particle translational velocities, $C_{vv}(t)$,

$$D = \frac{1}{3}\int_0^\infty C_{vv}(t)\, dt \tag{3}$$

The temperature dependence of the CIP diffusion coefficient was fitted to the Arrhenius equation,

$$D = A\cdot\exp(-b/T) \tag{4}$$

which follows from the Vogel−Tamman−Fulcher theory.[36]

Results and Discussion

Energy Exchange Times. The characteristic time scales of the vibrational energy transfer among the (14, 14) CNT, CIP molecule, and water, corresponding to system I in Table 1, are shown in Table 3. The corresponding ACFs of the interaction energies are shown in Figure 2. All fast components of energy transfer are considerably shorter than 1 ps. The slow components are also relatively short, less than 10 ps. Generally, the fast and slow time scales correspond to independent and collective vibrational motions.[37,38] In the case of water, the fast component can be described by interactions of individual and uncoupled water molecules with CIP and CNT, whereas the slow component is due to diffusion motions involving multiple water molecules. Correspondingly, uncoupled normal vibrational modes of CIP and CNT are responsible for the faster response, and the slower response is facilitated by coupling between the modes.

The fast relaxation component is responsible for over 50% of energy transferred by the CIP−CNT, CNT−water, and CIP−water interactions. These results are in good agreement with the outcomes of our earlier studies of the vibrational energy transfer between CNT and water in the absence of a drug molecule.[39] The CNT−water energy transfer exhibits a subpicosecond and a sub-10-ps time scale in both the presence and the absence of a drug molecule. However, the longer time scale shows larger amplitude in the presence of the molecule, likely due to the disruption of the water hydrogen-bonding structure by the molecule and more random interactions between waters, accelerating transition to the diffusive response.[37]

The fastest energy transfer occurs between water and CIP due to their strong electrostatic interaction and close contact. Therefore, energy lost by CNT will be rapidly equilibrated between CIP and water. The average energy of the Coulomb interaction between water and CIP is almost 2 orders of magnitude stronger than the Lennard-Jones interaction. The corresponding values are −3664 and −56.8 kJ/mol. In turn, the exchange of the Coulomb interaction energy is about three times faster than the exchange of the Lennard-Jones energy. Since the fast and slow energy exchange time scales are shorter for the CNT−CIP pair than for the CNT−water pair and since the

TABLE 3: Energy Transfer Time Scales and Amplitudes, eq 2, Calculated for System I at 298 K[a]

	CNT−CIP	CNT−H_2O	CIP−H_2O (C)	CIP−H_2O (LJ)
A	76%	52%	73%	83%
t_{fast} (ps)	0.08	0.14	0.06	0.27
t_{slow} (ps)	5.09	6.21	2.04	5.56

[a] See Table 1 for the system designation.

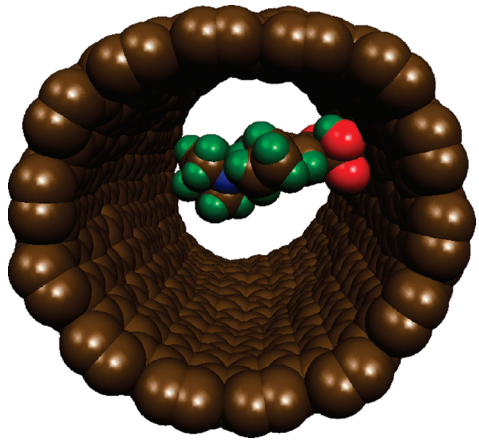

Figure 3. An instantaneous configuration of equilibrated system I, defined in Table 1. Water molecules have been removed for clarity.

amplitude of the fast energy exchange component is larger for the CNT−CIP than CNT−water interaction, 76% vs 52% (see Table 3), one can conclude that the CIP molecule interacts with the carbon atoms of the nanotube directly.

To investigate the nature of the CNT-CIP interaction, we analyzed the MD trajectory to establish the orientation of the CIP molecule as it approaches the CNT. A priori, one could expect a strong coupling between the π-electronic systems of CIP and CNT, resulting in a flat adsorption of the molecule on the tube wall. Surprisingly, in the majority of cases, the CIP molecule approached the CNT with its carboxylic acid end (see Figure 3). This situation was observed with both (14, 14), shown in Figure 3, and (30, 30) tubes, and can be rationalized by the direction of the CIP dipole moment (Figure 1a) that influences the CIP−water interactions. Generally, the electrostatic potential created by a dipole moment is much stronger in the direction of the dipole rather than perpendicular to it. Hence, the CIP−water interaction is also strongest for water molecules situated along the dipole direction. The number of such molecules is maximized if the dipole points along the tube axis. As a result, the molecule orients itself perpendicular to the tube axis and approaches the tube with one of its rim atoms. The preference for the carboxylic group orientation toward the tube may be rationalized by the particularly large value of the negative charge on the [22N] atom at the opposite end of the molecule, pointing into the solvent.

The CIP-CNT interaction is notably weakened in the presence of multiple CIP molecules, which tend to form clusters due to the strong antiferroelectric correlations between the molecular dipole moments.[40,41] The clusters tend to aggregate in the middle of the tube (Figure 1b).

The times of all energy transfer processes in the investigated systems are much shorter than any of the processes taking place in biological cells. Earlier studies have shown that the NIR excitation of the electronic degrees of freedom of CNTs and the electron-vibrational energy transfer are also ultrafast, taking place within hundreds of femtoseconds.[25,42−44] These facts clearly favor efficient heat-driven release of drug molecules from the CNTs.

Rapid energy exchange between NIR-activated CNTs and their surroundings is favorable for other medical applications of CNTs. For instance, endocytosis is known to rely on incorporation of molecules inside endosomes or lipid vesicles during and after cell entry.[45] Incorporation and subsequent heating of CNTs inside malignant endosomes will result in endosome destruction. The effectiveness of the interaction of the NIR light with DNA−CNT complexes[46] after endocytosis for endosomal rupture has already been used for efficient drug delivery.[27]

Diffusion Coefficient. Heat-induced release of the encapsulated drug molecule requires enhanced diffusion of the molecule at an elevated temperature. To investigate the temperature dependence of the diffusion coefficient of the encapsulated CIP molecule, we performed the MD simulations at six temperatures ranging from 278 to 363 K (Figure 4a). The lower temperatures represent the drug storage and delivery regime, and the higher temperatures correspond to CNT heating and drug release. The temperature of 310 K (37 °C) is of primary biological importance, since it is the temperature of the human body.

The diffusion coefficients are comparatively low for CIP inside the (14, 14) CNT at 278 and 298 K, 0.21 and 0.35 $\times$ 10^{-9} m^2/s, respectively. For comparison, the diffusion coefficients of most ions in dilute aqueous solutions are in the range of 0.6 $\times$ 10^{-9} to 2 $\times$ 10^{-9} m^2/s at room temperature. For large biological molecules, the diffusion coefficients normally range from 10^{-11} to 10^{-10} m^2/s. The relatively low diffusion coefficient of CIP is the result of its large atomic mass, branched structure, and high polarity. The CIP dipole moment is 13.9 D, resulting in a strong interaction with water and solvation shells that are fairly tightly bound to the solute. As the temperature rises to 363 K, the diffusion coefficient grows substantially and becomes almost 5 times higher, 1.02 $\times$ 10^{-9} m^2/s.

The strong temperature dependence of the diffusion coefficient of the CIP molecule is evidently due to its hydrophilic properties. Elevating the temperature not only speeds up the CIP motion directly but also loosens and sheds some of the solvent molecules that were more tightly bound to CIP at low temperatures, thereby decreasing the CIP effective mass. The CIP diffusion coefficient exhibits exponential temperature dependence, which follows from the Vogel−Tamman−Fulcher equation and that can be fit well to the Arrhenius equation, eq 4. The fitting parameters and correlation coefficients R for the CIP solutions of different concentrations are summarized in Table 4.

The rapid increase in the CIP diffusion coefficient with temperature favors the heat-driven release of the drug. The observed tendency suggests that the NIR control over the drug encapsulation inside CNTs can be achieved to a large extent through the temperature dependence of the diffusion coefficient. It may not be necessary, for instance, to raise the local temperature inside CNTs to the point of evaporation of the confined solution. At the same time, the value of the diffusion coefficient at body temperature is not sufficiently low for keeping the drug inside the CNT during the drug delivery stage. Hence, CNT capping is required during CNT tissue penetration.[11] It has been suggested[12] that drugs can be stored inside CNTs in a solid phase. In this case, CNT heating will considerably accelerate drug release due to both the growth of the diffusion coefficient and the expected increase of the local drug solubility at elevated temperatures. Although the diffusion

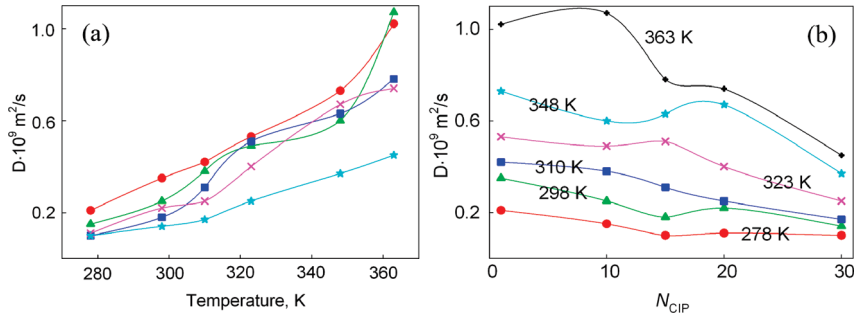

Figure 4. Diffusion coefficients of CIP molecules vs (a) temperature and (b) concentration. The data in part (a) correspond to system I (red circles), II (green triangles), III (blue squares), IV (pink crosses), and V (light blue stars). See Table 1 for the definition of the systems.

TABLE 4: Parameters of the Arrhenius Equation, eq 4, Describing Temperature Dependence of the Diffusion Coefficients of the CIP Molecules[a]

system	A (10^{-9} m^2/s)	b	R^b, %
I	150.4	1826	99.7
II	539.5	2288	93.7
III	209.7	2019	95.0
IV	270.2	2122	97.6
V	84.93	1898	99.4

[a] See Table 1 for the system designations. [b] R is a coefficient of correlation between molecular dynamics data and fitting curve.

constants were obtained for rather short tubes, they can be used directly to predict the release of CIP for tubes of arbitrary lengths, since CNTs are uniform along its axial direction.

The size of the (14, 14) CNT was chosen to allow comfortable CIP fit inside the tube, regardless of CIP orientation. Loading a single drug molecule per CNT may not be so efficient for medical purposes. Medical applications require relatively large amounts of drugs. For instance, a considerable number of CIP molecules are required to kill a single bacterium. Hence, we investigated an alternative CNT−CIP design using a bigger (30, 30) CNT loaded with different amounts of CIP molecules. Generally, a larger number of drug molecules per CNT should result in a higher medical efficiency. Systems II−V contain solutions of confined CIP with concentrations from 0.2 to ~0.5 mol/L (Table 1).

Figure 4b shows the concentration dependence of the CIP diffusion coefficient. Higher concentrations decrease the diffusion coefficient, most likely due to interactions between the CIP molecules, resulting in a larger CIP effective mass. Both direct long-range coupling between the CIP dipoles and indirect interactions through polarization of water structure by the polar CIP molecules are possible. An increase in the media polarity would naturally decrease the diffusion rate. This is true for increased polarity of both solvent and solute molecules. In addition, the temperature dependence of the diffusion constant should become stronger in more polar media, since the interaction energy term entering the Arrhenius expression, b in eq 4, will be larger. Accordingly, the trends should reverse in the less polar and nonpolar solvents.

The present model is limited only to the protonated state of the CIP molecule, although its water solution should contain generally deprotonated $-COO^-$ groups. For the studied properties, this does not produce artifacts, since both diffusion and energy transfer depend mostly on the intermolecular interactions, which should not be significantly changed due to the deprotonation process in solution. To prove this point, we computed the distribution of atomic charges for the deprotonated CIP and found that the overall charge distribution changed little. Only the charges on the atoms of and close to the carboxyl group were affected by the deprotonation. Since the strongest interactions that govern CIP diffusion are Coulomb interactions in CIP−CIP and CIP−water pairs, the above finding allowed us to conclude that the deprotonation of CIP should not significantly affect the CIP diffusion coefficient.

The concentration dependence of the diffusion coefficient is more pronounced at higher temperatures (Figure 4b). At the same time, the diffusion coefficient is more sensitive to temperature at the lower concentration(Figure 4a). The parameters of the Arrhenius fit, eq 4 and Table 4, to the temperature dependence of the CIP diffusion coefficient are generally similar in the (14, 14) CNT and (30, 30) CNT systems for all CIP loadings, indicating that the activation mechanism of CIP diffusion according to the Vogel−Tamman−Fulcher theory remains the same in all cases. The correlation coefficients for the fits are quite high, proving that all observed temperature dependences are exponential.

The small deviations from the exponential behavior (Figure 4) can be attributed to the thermal fluctuations in the systems. The deviations can also be due to general uncertainties of the diffusion constants. These uncertainties can be quite high. The degree of CIP loading inside CNT should not significantly influence the effectiveness of the heat-driven drug release. We also believe that the observed concentration dependence of the diffusion coefficient is less important for the drug release process than the temperature dependence. Laser-induced heating of the solvent inside the tube can be quite significant, in particular if the radiation is applied continuously. The change in the diffusion constant over the temperature range between 278 and 363 K is more significant than the factor-of-2 change due to the concentration differences. Further, the factor-of-2 change due to the concentration differences is sufficiently small to eliminate the possibility of phase-transition-like phenomena.

Conclusions

To reiterate, vibrational energy transfer among CNT, water, and CIP takes place within 10 ps or less, which is much faster than the time scales of relevant biological processes. This fact is very positive for the proposed heat-driven drug release mechanism. The low diffusion coefficient of the CIP molecules confined inside CNTs at all investigated concentrations is favorable for CIP storage and delivery. The 5-to-7-fold-growth of the CIP diffusion coefficient within the temperature range from 278 to 363 K for all CIP concentrations suggests that CNT heating by NIR radiation can potentially be used for effective drug release.

Acknowledgment. The authors are grateful to Tammie Nelson for comments on the manuscript. O.V.P. acknowledges

financial support of DOE, Grant DE-FG02-05ER15755, and ACS PRF, Grant 41436-AC6.

References and Notes

(1) Zhang, L. W.; Zeng, L.; Barron, A. R.; Monteiro-Riviere, N. A. *Int. J. Toxicol.* **2007**, *26* (2), 103–13.

(2) Liu, Z.; Davis, C.; Cai, W.; He, L.; Chen, X.; Dai, H. *Proc. Natl. Acad. Sci. U.S.A.* **2008**, *105* (5), 1410–5.

(3) Liu, Z.; Cai, W.; He, L.; Nakayama, N.; Chen, K.; Sun, X.; Chen, X.; Dai, H. *Nat. Nanotechnol.* **2007**, *2* (1), 47–52.

(4) Singh, R.; Pantarotto, D.; Lacerda, L.; Pastorin, G.; Klumpp, C.; Prato, M.; Bianco, A.; Kostarelos, K. *Proc. Natl. Acad. Sci. U.S.A.* **2006**, *103* (9), 3357–62.

(5) Wang, H.; Wang, J.; Deng, X.; Sun, H.; Shi, Z.; Gu, Z.; Liu, Y.; Zhao, Y. *J. Nanosci. Nanotechnol.* **2004**, *4* (8), 1019–24.

(6) Aillon, K. L.; Xie, Y.; El-Gendy, N.; Berkland, C. J.; Forrest, M. L. *Adv. Drug Delivery Rev.* **2009**, *61* (6), 457–66.

(7) Hilder, T. A.; Hill, J. M. *Small* **2009**, *5* (3), 300–8.

(8) Bhirde, A. A.; Patel, V.; Gavard, J.; Zhang, G.; Sousa, A. A.; Masedunskas, A.; Leapman, R. D.; Weigert, R.; Gutkind, J. S.; Rusling, J. F. *ACS Nano* **2009**, *3* (2), 307–16.

(9) Dhar, S.; Liu, Z.; Thomale, J.; Dai, H.; Lippard, S. J. *J. Am. Chem. Soc.* **2008**, *130* (34), 11467–76.

(10) Weng, X.; Wang, M.; Ge, J.; Yu, S.; Liu, B.; Zhong, J.; Kong, J. *Mol. Biosyst.* **2009**, *5* (10), 1224–31.

(11) Hillebrenner, H.; Buyukserin, F.; Kang, M.; Mota, M. O.; Stewart, J. D.; Martin, C. R. *J. Am. Chem. Soc.* **2006**, *128* (13), 4236–7.

(12) Ajima, K.; Yudasaka, M.; Murakami, T.; Maigne, A.; Shiba, K.; Iijima, S. *Mol. Pharm.* **2005**, *2* (6), 475–80.

(13) Son, S. J.; Bai, X.; Nan, A.; Ghandehari, H.; Lee, S. B. *J. Controlled Release* **2006**, *114* (2), 143–52.

(14) Mintzer, M. A.; Simanek, E. E. *Chem. Rev.* **2009**, *109* (2), 259–302.

(15) Ko, S.; Liu, H.; Chen, Y.; Mao, C. *Biomacromolecules* **2008**, *9* (11), 3039–43.

(16) Kumar, A.; Jena, P. K.; et al. *J. Biomed. Nanotechnol.* **2005**, *1* (4), 392–6.

(17) Riggio, C.; Ciofani, G.; et al. *Res. Lett.* **2009**, *4* (7), 668–673.

(18) Liu, Z.; Sun, X.; Nakayama-Ratchford, N.; Dai, H. *ACS Nano* **2007**, *1* (1), 50–6.

(19) Liu, Z.; Chen, K.; Davis, C.; Sherlock, S.; Cao, Q.; Chen, X.; Dai, H. *Cancer Res.* **2008**, *68* (16), 6652–60.

(20) Wu, W.; Wieckowski, S.; Pastorin, G.; Benincasa, M.; Klumpp, C.; Briand, J. P.; Gennaro, R.; Prato, M.; Bianco, A. *Angew. Chem., Int. Ed.* **2005**, *44* (39), 6358–62.

(21) Sung, J.; Barone, P. W.; Kong, H.; Strano, M. S. *Biomaterials* **2009**, *30* (4), 622–31.

(22) Popov, A. M.; Lozovik, Y. E.; Fiorito, S.; Yahia, L. *Int. J. Nanomed.* **2007**, *2* (3), 361–72.

(23) Klingeler, R.; Hampel, S.; Buchner, B. *Int. J. Hypertherm.* **2008**, *24* (6), 496–505.

(24) Cheng, Y.; Pei, Q. X.; Gao, H. *Nanotechnology* **2009**, *20* (14), 145101.

(25) Carlson, L. J.; Krauss, T. D. *Acc. Chem. Res.* **2008**, *41* (2), 235–43.

(26) O'Connell, M. J.; Bachilo, S. M.; Huffman, C. B.; Moore, V. C.; Strano, M. S.; Haroz, E. H.; Rialon, K. L.; Boul, P. J.; Noon, W. H.; Kittrell, C.; Ma, J.; Hauge, R. H.; Weisman, R. B.; Smalley, R. E. *Science* **2002**, *297* (5581), 593–6.

(27) Kam, N. W.; O'Connell, M.; Wisdom, J. A.; Dai, H. *Proc. Natl. Acad. Sci. U.S.A.* **2005**, *102* (33), 11600–5.

(28) Mitscher, L. A. *Chem. Rev.* **2005**, *105* (2), 559–92.

(29) Van Der Spoel, D.; Lindahl, E.; Hess, B.; Groenhof, G.; Mark, A. E.; Berendsen, H. J. GROMACS: fast, flexible, and free. *J. Comput. Chem.* **2005**, *26* (16), 1701–18.

(30) van Gunsteren, W. F.; Billeter, S. R.; Eising, A. A.; Hünenberger, P. H.; Krüger, P.; Mark, A. E.; Scott, W. R. P., Tironi, I. G. *Biomolecular Simulation: The GROMOS96 Manual and User Guide*; vdf Hochschulverlag AG an der ETH Zürich and BIOMOS b.v.: Zürich, Switzerland, 1996.

(31) Berendsen, H. J. C.; Grigera, J. R.; Straatsma, T. P. *J. Phys. Chem.* **1987**, *91* (24), 6269–71.

(32) Breneman, C. M.; Wiberg, K. B. *J. Comput. Chem.* **1990**, *11*, 361–73.

(33) Allen, M. P.; Tildesley, D. J. *Computer Simulation of Liquids;* Oxford University Press: New York, 1987.

(34) Van Der Spoel, D.; Lindahl, E.; Hess, B.; van Buuren, A. R.; Apo, E.; Meulenhoff, P. J.; Tieleman, D. P.; Sijbers, A. L. T. M.; Feenstra, K. A.; van Drunen, R.; Berendsen, H. J. C. *Cromacs User Manual version 4.0*; 2005. http://www.gromacs.org/@api/deki/files/82/=gromacs4_manual.pdf.

(35) Parrinello, M.; Rahman, A. R. *J. Appl. Phys.* **1981**, *52*, 7182–90.

(36) Vogel, H. *Phys. Z.* **1921**, *22*, 645.

(37) Brooksby, C.; Prezhdo, O. V.; Reid, P. J. *J. Chem. Phys.* **2003**, *118*, 4563–72.

(38) Bragg, A. E.; Cavanagh, M. C.; Schwartz, B. J. *Science* **2008**, *321* (5897), 1817–22.

(39) Nelson, T. R.; Chaban, V. V.; Kalugin, O. N.; Prezhdo, O. V. *J. Phys. Chem. B* **2010**, *114* (13), 4609–14.

(40) Pereverzev, Y. V.; Prezhdo, O. V.; Dalton, L. R. *ChemPhysChem* **2004**, *5* (12), 1821–30.

(41) Pereverzev, Y. V.; Prezhdo, O. V.; Dalton, L. R. *Phys. Rev. B* **2002**, *65*, 052104.

(42) Luer, L.; Gadermaier, C.; Crochet, J.; Hertel, T.; Brida, D.; Lanzani, G. *Phys. Rev. Lett.* **2009**, *102* (12), 127401.

(43) Habenicht, B. F.; Craig, C. F.; Prezhdo, O. V. *Phys. Rev. Lett.* **2006**, *96* (18), 187401.

(44) Habenicht, B. F.; Kamisaka, H.; Yamashita, K.; Prezhdo, O. V. *Nano Lett.* **2007**, *7* (11), 3260–5.

(45) Mukherjee, S.; Ghosh, R. N.; Maxfield, F. R. Endocytosis. *Physiol. Rev.* **1997**, *77* (3), 759–803.

(46) Yarotski, D. A.; Kilina, S. V.; Talin, A. A.; Tretiak, S.; Prezhdo, O. V.; Balatsky, A. V.; Taylor, A. J. *Nano Lett* **2009**, *9* (1), 12–17.

JP104507G